Talanta 283 (2025) 127166

Contents lists available at ScienceDirect

Talanta

journal homepage: www.elsevier.com/locate/talanta

A colorimetric and SERS-based LFIA for sensitive and simultaneous detection of three stroke biomarkers: An ultra-fast and sensitive point-of-care testing platform

Yutong Wang [a,1], Qianchun Zhang [c,1], Mengping Huang [a], Ganggang Ai [a], Xiaofeng Liu [d], Yuqi Zhang [a,***], Ran Li [a,*], Jie Wu [b,**]

[a] Yan'an Key Laboratory of Green Chemical Energy, Key Laboratory of New Energy & New Functional Materials, National Center for Quality supervision and Inspection of Oil and Gas products (Yan'an), College of Chemistry and Chemical Engineering, Yan'an University, Yan'an, 716000, China
[b] School of Public Health, Shenyang Medical College, Liaoning Medical Functional Food Professional Technology Innovation Center, Shenyang, 110034, China
[c] School of Biology and Chemistry, Key Laboratory for Analytical Science of Food and Environment Pollution of Qianxinan, Xingyi Normal University for Nationalities, Xingyi, 562400, China
[d] Guangxi Key Laboratory of Urban Water Environment, Baise University, Baise, 533000, China

ARTICLE INFO

Keywords:
Colorimetric
SERS
LFIA
POCT
Ultra-fast
Simultaneous detection

ABSTRACT

Stroke ranks as the second leading cause of disability and mortality globally. Biomarker detection represents a promising avenue for predicting disease severity and prognosis. The expression levels of metalloproteinase-9 (MMP-9), neuron-specific enolase (NSE), and N-terminal pro-brain natriuretic peptide (NT-pro BNP) in blood correlate with stroke severity. Hence, monitoring these biomarkers is crucial for stroke diagnosis and management. Point-of-care testing (POCT) offers on-site diagnostic capabilities, with lateral flow immunoassay (LFIA) being the most widely used method currently. However, traditional LFIA sensitivity requires enhancement. This study introduces an ultra-sensitive surface-enhanced Raman scattering-based lateral flow immunoassay (SERS-based LFIA) strip for simultaneous detection of the three stroke biomarkers using SERS immune tags. Bimetallic core-shell structured SERS immune tags leverage the advantages of two metals, ensuring stability and enhancing Raman signals through plasmon resonance. This development of a POCT based on SERS-based LFIA strips offers rapid, sensitive, and multiplex detection of stroke biomarkers. The limits of detection (LODs) for MMP-9, NSE, and NT-pro BNP were 0.00020 ng mL^{-1}, 0.00016 ng mL^{-1}, and 0.00012 ng mL^{-1}, respectively. Furthermore, enzyme-linked immunosorbent assay (ELISA) validated the accuracy of SERS-based LFIA. Clinical sample analysis demonstrated consistency between outcomes obtained by SERS-based LFIA and ELISA. Thus, SERS-based LFIA presents a novel POCT approach for stroke diagnosis.

1. Introduction

Stroke represents a global health crisis and is the second leading cause of death worldwide, resulting in significant disability and imposing substantial economic burdens [1–3]. The World Stroke Organization and Lancet Neurology Commission have projected a 50 % increase in stroke mortality from 2020 to 2050 [4]. Consequently, there has been a call from the World Stroke Organization and the World Federation of Neurology to revise guidelines for primary stroke and cardiovascular disease prevention, emphasizing early detection strategies for adults at any risk level [5]. Currently, stroke diagnosis primarily relies on clinical evaluation supplemented by diagnostic and imaging tools. Commonly, neurological assessments employ scoring systems such as the National Institutes of Health Stroke Scale (NIHSS) [6]. While computed tomography (CT) and magnetic resonance imaging (MRI) serve as gold standards [7,8] for stroke diagnosis, NIHSS exhibits low sensitivity, and CT and MRI have limitations that hinder immediate detection [9–11]. Therefore, urgent development of methods enabling

* Corresponding author.
** Corresponding author.
*** Corresponding author.
E-mail addresses: yqzhang@iccas.ac.cn (Y. Zhang), lirandeqhd@vip.163.com (R. Li), wujie072@163.com (J. Wu).
[1] Yutong Wang and Qianchun Zhang contributed equally to this work.

https://doi.org/10.1016/j.talanta.2024.127166
Received 3 September 2024; Received in revised form 28 October 2024; Accepted 4 November 2024
Available online 6 November 2024

rapid stroke diagnosis and recognition is imperative.

Biomarkers, which are indicators found in body fluids and tissues, offer a promising avenue for predicting physiological and disease states [12–14]. Recently, detection of stroke biomarkers such as matrix metalloproteinase-9 (MMP-9) [15], neuron-specific enolase (NSE) [16], and N-terminal pro-brain natriuretic peptide (NT-pro BNP) [17,18] has provided an alternative approach for swift stroke diagnosis. The expression levels of these biomarkers in blood correlate with stroke severity, highlighting the critical importance of their facile and sensitive monitoring for stroke diagnosis and management. Therefore, it is essential to develop a method that can detect multiple biomarkers simultaneously and with high sensitivity.

Point-of-care testing (POCT) refers to on-site testing systems that provide immediate diagnostic and treatment information at the bedside [19,20], proving highly practical in disease diagnosis. The most prevalent POCT method currently is lateral flow immunoassay (LFIA) [21], valued for its portability, rapidity, cost-effectiveness, and ease of use [22–24]. However, conventional LFIA suffers from poor sensitivity, limiting its utility to qualitative rather than quantitative detection [25–27], which has spurred efforts toward signal amplification and quantification in LFIA development [28–30]. Surface-enhanced Raman scattering (SERS) offers a solution, leveraging its ability to vastly amplify Raman signals from target molecules. This highly sensitive technique has been widely applied in chemical and biomedical analyses due to its capability to enhance sensitivity even at the single-molecule level and to provide unique molecular fingerprint information [31, 32]. Integration of SERS with LFIA represents a promising advancement. SERS-based LFIA combines the high sensitivity and specificity of SERS with the simplicity and rapidity of LFIA, and it has the multiple detection ability. These advantages make it ideal choice for clinical POCT that can achieve multiple and sensitive detection. Recent research [33–36] has demonstrated sensitive quantitative analysis of viruses, bacteria, protein toxins, infection biomarkers, and other targets using SERS-based LFIA, underscoring its potential for stroke diagnosis and prediction.

Given the multifaceted etiology of stroke and the low abundance of blood biomarkers, a straightforward, rapid, and accurate method for simultaneous detection of multiple stroke markers would significantly enhance stroke diagnosis and prediction. Here, the SERS-based LFIA strips as an in vitro diagnostic and POCT method was developed and analyzed serum samples from 12 stroke patients. In this paper, Au@Ag core-shell nanoparticles were synthesized to exploit the advantages of both metals, enhancing stability and expanding the excitation spectrum to facilitate plasmon resonance coupling. 5,5′-Dithiobis-(2-nitrobenzoic acid) (DTNB) was employed as a Raman reporter, and Au@Ag NPs@DTNB was prepared and conjugated with labeled antibodies to form SERS immune tags (Au@Ag NPs@DTNB-labeled antibodies). These SERS immune tags exhibited robust SERS signals, accuracy, and exceptional stability in SERS-based LFIA. And, the enzyme-linked immunosorbent assay (ELISA) was used to validate the accuracy of SERS-based LFIA, and the results of the two methods were basically consistent. These results indicate that SERS-based LFIA can detect MMP-9, NSE and NT-pro BNP rapidly, sensitively and multiplex. This highly sensitive and effective immunoassay based on SERS-based LFIA has potential become a novel approach for POCT diagnosis of stroke, and promote the development of SERS in biological detection.

2. Experimental section

2.1. Reagents and materials

Gold (III) chloride trihydrate ($HAuCl_4{\cdot}3H_2O$), hexadecyltrimethylammonium bromide (CTAB), and L-ascorbic acid (AA) were purchased from Sigma-Aldrich. Silver nitrate ($AgNO_3$), polyvinylpyrrolidone (PVP), 5,5′-Dithiobis-(2-nitrobenzoic acid) (DTNB), sucrose, Tween-20, and trisodium citrate dihydrate were purchased from Aladdin. Bovine serum albumin (BSA) was obtained from Rhawn. Hydrochloric acid (HCl) and sodium hydroxide (NaOH) were supplied by Tianjin Kemiou Chemical Reagent Co., Ltd. Phosphate-buffered saline (PBS, pH = 7.4, 20 mM) was prepared by mixing stock solutions of NaH_2PO_4 (20 mM) and Na_2HPO_4 (20 mM), and served as the buffer solution. Ultrapure water (18.2 MΩ cm^{-1}) from a Milli-Q water purifying system was used as the solvent in all experiments unless otherwise specified.

Neuron-specific enolase (NSE) standard grade antigens, N-terminal prohormone of brain natriuretic peptide (NT-pro BNP) standard grade antigens, anti-NSE McAb (labeling antibody), anti-NSE McAb (coating antibody), anti-NT-pro BNP McAb (labeling antibody), anti-NT-pro BNP McAb (coating antibody), and Goat Antibody to mouse Immunoglobulin G (IgG) were purchased from Linc-Bio Science Co., Ltd. (Shanghai, China). Matrix metalloproteinase-9 (MMP-9) standard grade antigens, anti-MMP-9 McAb (labeling antibody), anti-MMP-9 McAb (coating antibody), MMP-9 ELISA kit, NSE ELISA kit, and NT-pro BNP ELISA kit were obtained from UpingBio Technology Co., Ltd. (Shenzhen, China). Nitrocellulose (NC) membranes (CN 95, CN 140) were sourced from Sartorius (Germany). The NC membrane (Pall vivid 120, PALL 120), sample pad (XQ-Y8), absorbent pad (H5072), conjugate pad (GL0194), and polyvinyl chloride (PVC) plate (DB-6) were purchased from Shanghai Jieyi Biotechnology Co., Ltd. (China).

2.2. Preparation of human serum samples

Serum samples from stroke patients and healthy individuals were collected at the Heart, Brain & Vascular Hospital of Yanan University Affiliated Hospital and stored at −80 °C until use. Informed consent was obtained from all participants, and the study protocol was approved by the Ethics Committee of the Yanan University Affiliated Hospital.

2.3. Instruments

Transmission electron microscopy (TEM) analyses were conducted using a JEM-F200 electron microscope operating at 200 kV (JEOL, Japan). Energy-dispersive spectroscopy (EDS) for element characterization was performed in dark-field scanning transmission electron microscopy (STEM) mode on the TEM. UV–Vis absorption spectra were recorded on a UV-2550 spectrometer (Shimadzu, Japan). Zeta potential measurements were carried out using a Zetasizer Nano ZS90 zeta potential analyzer (Malvern, UK). Lateral flow immunoassay test strips were prepared using an XYZ platform dispenser HM 3035 from Shanghai Kinbio Tech. Co., Ltd. SERS spectra were recorded using a LabRam Soleil Raman microscope (Horiba, France) equipped with a 638 nm excitation laser.

2.4. Synthesis of Au@Ag NPs

Gold seed preparation involved adding 7.5 mL of 1 % trisodium citrate dihydrate to 50 mL of boiling 1 mM $HAuCl_4{\cdot}3H_2O$ solution, boiling for 15 min, cooling to room temperature, and storing at 4 °C. For Au@Ag NPs synthesis, 600 μL of the above gold seed was added to a 60 mL solution of 0.25 mM $HAuCl_4{\cdot}3H_2O$ containing 60 μL of 1 M HCl, followed by addition of 300 μL of 0.1 M AA and 600 μL of 3 mM $AgNO_3$ under stirring at room temperature. After stirred for 30 s, 2 mL of 0.2 M CTAB was added to stabilize the particles during centrifugation. After one centrifugal wash at 6000 rpm for 15 min, the solution was redispersed in 2 mM CTAB. 360 μL of 0.1 M AA, 60 μL of 0.1 M $AgNO_3$, and 450 μL of 0.1 M NaOH were added, followed by stirring for 30 min, centrifugation, and redispersion in 60 mL of 2 mM CTAB, for storage at 4 °C.

2.5. Preparation of stroke biomarkers labeling antibody modified Au@Ag NPs@DTNB SERS immune tags

To prepare Au@Ag NPs@DTNB, 100 μL of 10 mM DTNB Raman

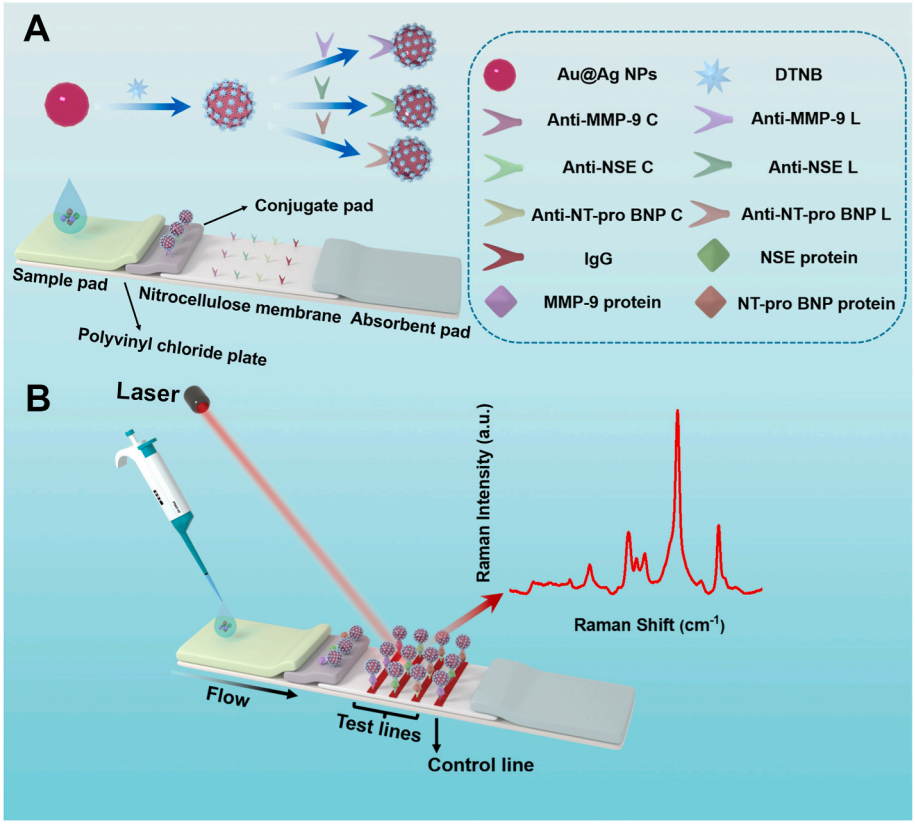

Fig. 1. Schematic diagram of the SERS-based LFIA strip for the detection of MMP-9, NSE and NT-pro BNP.

reporter was slowly added to 10 mL of Au@Ag NPs colloid, stirred overnight at 4 °C, centrifuged at 6000 rpm for 15 min, washed with ultrapure water, and redispersed in 3 mL of ultrapure water. The pH was adjusted to 8.0 with 0.1 M K_2CO_3. Au@Ag NPs@DTNB was then incubated with anti-MMP-9 McAb, anti-NSE McAb, and anti-NT-pro BNP McAb labeling antibodies (15 μg mL^{-1}) for 2 h at 4 °C. BSA (1 %, w/v) was added to block nonspecific sites, followed by centrifugation and washing with PBS buffer three times. The SERS immune tags were stored in eluent buffer (20 mM PBS containing 0.5 % PVP, 2 % sucrose, 0.2 % BSA, and 0.05 % Tween-20) for future use.

2.6. Fabrication and immunoassay Procedure of the lateral flow test strip

The lateral flow test strip was assembled with a sample pad, NC membrane, conjugate pad, absorbent pad, and PVC plate. The sample pad was treated with 20 mM PBS containing 1 % BSA and 0.05 % Tween-20, dried overnight at 37 °C. Three coating antibodies (MMP-9, NSE, and NT-pro BNP) and IgG were sprayed onto the NC membrane as test line (T line, 1.0 mg mL^{-1}) and control line (C line, 1.0 mg mL^{-1}) at a rate of 1 μL cm^{-1}, dried at 37 °C for 1 h, and stored under dry conditions at room temperature. The three SERS immune tags were applied to the conjugate pad and dried similarly. The absorbent pad required no further modification. Components were assembled onto the PVC plate with a 2 mm overlap to ensure sample solution flow across the entire strip. The fully assembled card was cut into 4 mm-wide strips using a paper cutter and stored under dry conditions at room temperature for subsequent experiments. Lateral flow immunoassay (LFIA) for three stroke biomarkers involved applying 180 μL of sample solutions in running buffer (buffer containing 1.5 % BSA) onto the sample pad. Qualitative and quantitative measurements were obtained by observing the test line color and measuring Raman signal intensities of the test line after a few minutes. All experiments were conducted using at least three strip tests under the same conditions.

3. Results and discussion

3.1. Analysis Principle

The strategy employed SERS-based LFIA to detect three stroke biomarkers follows a typical sandwich immunoassay format (Fig. 1A). The target antigens, three biomarkers of stroke, were captured by Au@AgNPs@DTNB SERS immune tags, forming an immune complex. Through capillary action, this complex was subsequently immobilized by antibodies on the T-line, resulting in a sandwich complex formation that aggregated to produce visually discernible fuchsia lines. These immune reactions rely on specific binding between antigens and antibodies in the analytes. Excess SERS immune tags were captured by IgG on the C-line through nonspecific binding. Upon completion of the reaction, sandwich-structured compounds were observed on the T-line, enabling qualitative or quantitative analysis of antigens through detected SERS signals and observed color intensity on the T-line (Fig. 1B).

3.2. Synthesis and characterization of Au@Ag NPs and Au@Ag NPs@DTNB SERS immune tags

The synthesis of high-performance Au@Ag NPs was achieved via a facile seed-mediated growth method (Fig. 2A). And by detecting the intensity of DTNB at 1330 cm^{-1}, the enhancement factor of Au@Ag NPs substrate can be calculated was 3.07 × 10^8 (Fig. S1). TEM images initially revealed spherical Au NPs with an average size of 14.0 nm (Fig. 2B–D). Subsequently, these Au NPs served as seeds for the synthesis of Au@AgNPs using a one-step method. In the presence of NaOH, $AgNO_3$ was reduced by AA to form small Ag nanospheres that encapsulated the Au cores, resulting in Au@Ag NPs with a spherical shape and an average diameter of 50.5 nm (Fig. 2C–E). The d-spacing for adjacent lattice planes measured 0.235 nm and 0.223 nm (Fig. S2), corresponding to the (111) crystal plane of Au and the (102) crystal plane of Ag, respectively.

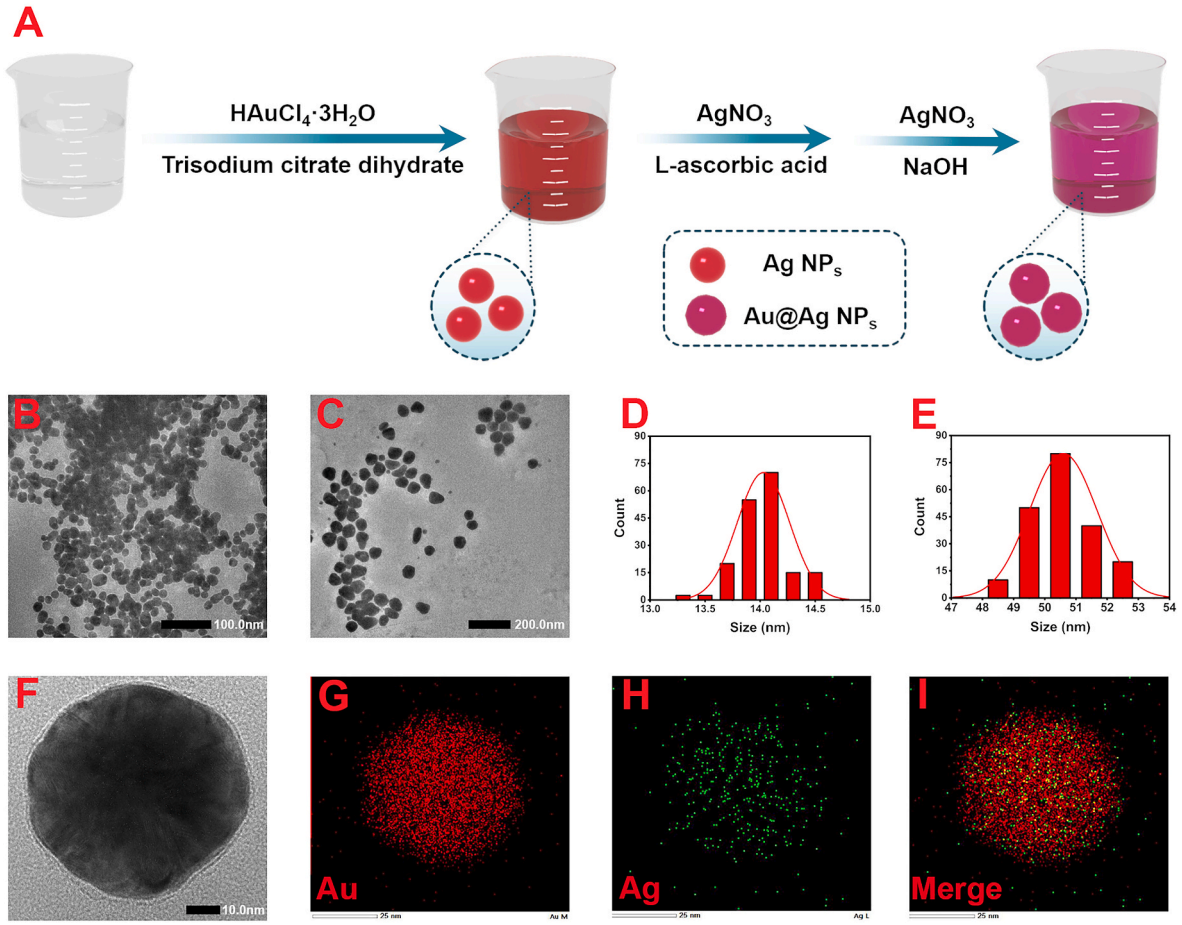

Fig. 2. Synthesis and characterization of Au Seeds and Au@Ag NPs. Schematic illustration of the synthetic process of Au Seeds and Au@Ag NPs (A); TEM images of Au Seeds (B), Au@Ag NPs (C); Hydrodynamic diameter of Au Seeds (D), Au@Ag NPs (E); Corresponding EDS elemental mapping of Au, Ag from Au@Ag NPs (F–I).

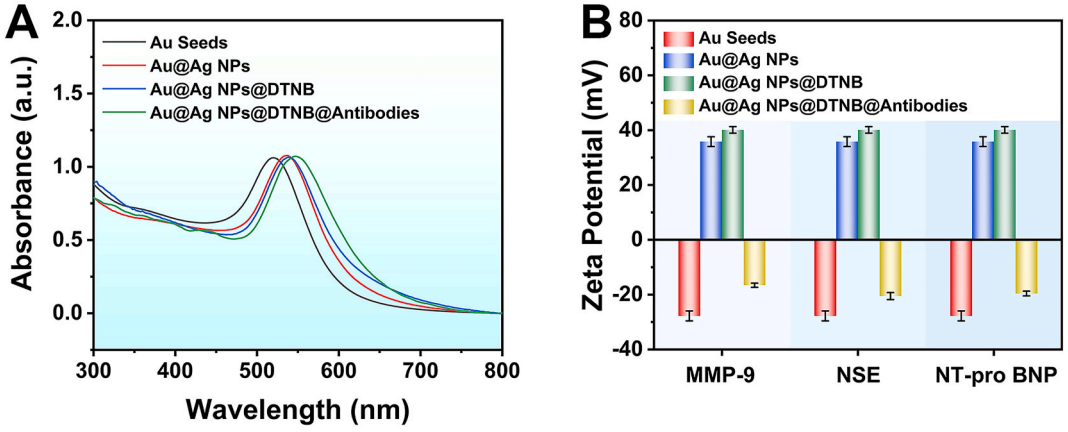

Fig. 3. UV–vis absorption spectra of the Au Seeds, Au@Ag NPs, Au@Ag NPs@DTNB, and Au@Ag NPs@DTNB@Antibodies (A); Zeta potential of different modified of Au Seeds surface (B–D).

Furthermore, elemental composition analysis via EDS mapping confirmed the successful assembly of Au@Ag NPs with a core-shell structure (Fig. 2F–I), where Au and Ag elements were marked in red and green, respectively.

The successful synthesis of Au@Ag NPs was further validated using UV–visible spectroscopy (Fig. 3A), which showed a shift in the localized surface plasmon resonance (LSPR) absorption band from 522 to 536 nm upon coating with Ag NPs. After incubation with DTNB to form Au@Ag NPs@DTNB, the LSPR absorption band exhibited a 2 nm red shift. Conjugation with anti-MMP-9 McAb, anti-NSE McAb, and anti-NT-pro BNP McAb resulted in a 12 nm red shift of the plasmon resonance peak, indicating successful antibody conjugation. Zeta potential measurements (Fig. 3B–D) confirmed different surface modifications of Au seeds: the zeta potential of Au@Ag NPs changed from 35.83 ± 1.80 mV to 40.10 ± 1.21 mV upon DTNB adsorption, and further shifted to −16.57 ± 0.76 mV, −20.53 ± 1.29 mV, and −19.6 ± 0.87 mV after conjugation with anti-MMP-9 McAb, anti-NSE McAb, and anti-NT-pro BNP McAb, respectively. These results collectively demonstrate the

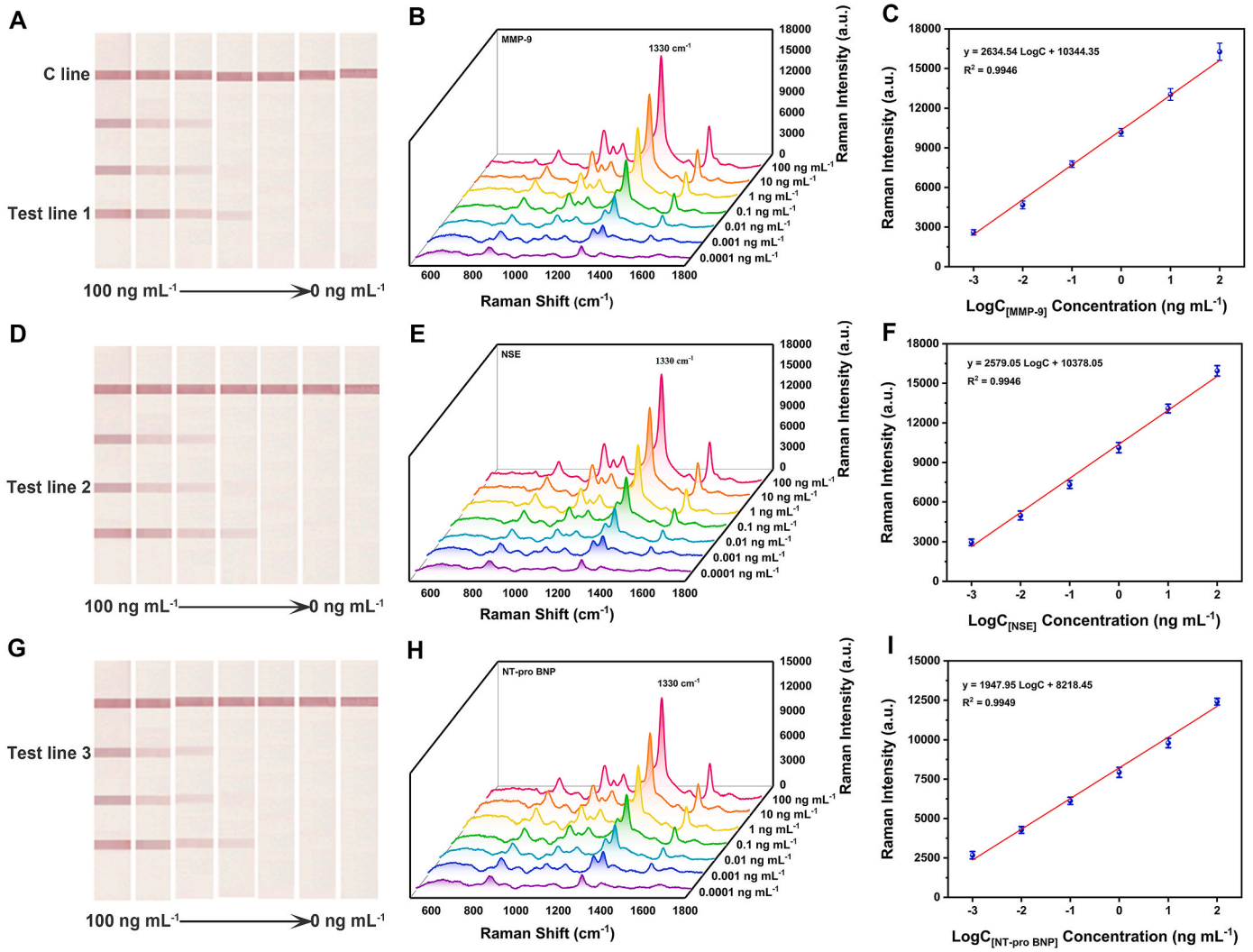

Fig. 4. Optical photographs (A–C) and corresponding SERS spectra of SERS-based LFIA strips at different concentrations of MMP-9, NSE and NT-pro BNP (D–F); Corresponding calibration lines of MMP-9, NSE and NT-pro BNP at SERS intensity of 1330 cm^{-1} (G–I).

successful synthesis of Au@Ag NPs and Au@Ag NPs@DTNB SERS immune tags. Besides, the use of PBS and BSA had no significant effect on the synthesis of Au@Ag NPs@DTNB SERS immune tags (Fig. S3).

3.3. Optimization of the immunoreaction conditions

To achieve high detection performance, several key parameters influencing LFIA performance was optimized using 100 ng mL^{-1} concentrations of three stroke biomarkers. Parameters such as sample pad, NC membrane, buffer composition, antibody coupling amount, and pH were evaluated for their effects on colorimetric and SERS signal intensities.

In the optimization process, the intensity of the SERS characteristic peak of DTNB at 1330 cm^{-1} was used to assess immunoreaction performance. The flow rate of the sample solution significantly affected antigen-antibody binding, influencing signal intensity and color shade. Flow rate, dictated by the NC membrane pore size, was tested using CN 95, PALL 120, and CN 140 membranes. Following completion of the immunoreaction, all three membranes effectively transported Au@Ag NPs@DTNB SERS tags (Fig. S4). However, CN 95 and PALL 120 membranes exhibited noticeable signal residue, while CN 140 membrane showed none, leading to its selection for further experiments.

Differences in fluorescence background on the NC membrane under various laser excitations were noted, potentially affecting SERS detection. Comparison of SERS signals under 532, 638, and 785 nm laser sources (Fig. S5) indicated higher fluorescence background on CN 140 membrane under 532 nm lasers, but lower SERS signals under 785 nm compared to 638 nm. Therefore, the 638 nm laser was chosen for subsequent SERS detection to ensure optimal sensitivity and minimize background interference.

Additionally, the antibody coupling amount and pH of Au@Ag NPs@DTNB solution were critical for stable antibody-SERS tag binding, directly influencing immunoreaction detection sensitivity. Antibody coupling amounts ranging from 5 to 20 μg mL^{-1} were tested, with 15 μg mL^{-1} chosen for subsequent experiments due to slightly higher Raman signal strength (Fig. S6). pH adjustments using K_2CO_3 (0.1 M) showed that pH 7.5 provided peak Raman intensity for the three antigens, with deviations noted at pH 8.0 (Fig. S7), confirming pH 7.5 as optimal for antibody coupling.

3.4. Analytical performance of three stroke biomarkers detection with SERS-based LFIA

Under optimized conditions, the detection performance of SERS-based LFIA was evaluated by analyzing MMP-9, NSE, and NT-pro BNP samples at various concentrations (0.001–100 ng mL^{-1}) using both colorimetric signals and Raman intensity modes. Optical photographs (Fig. 4A–C) demonstrated gradual reduction in T-line color intensity

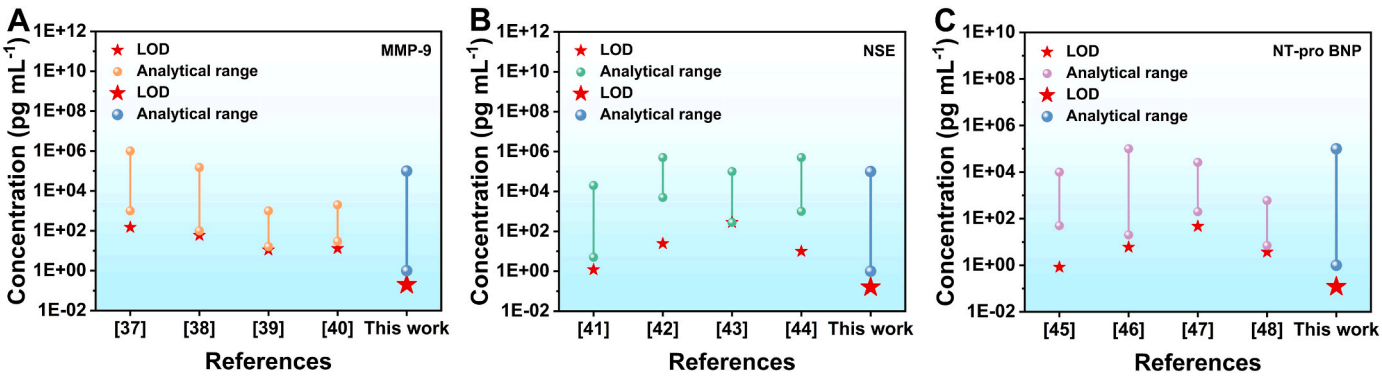

Fig. 5. Compared with some recently other methods for stroke biomarkers detection.

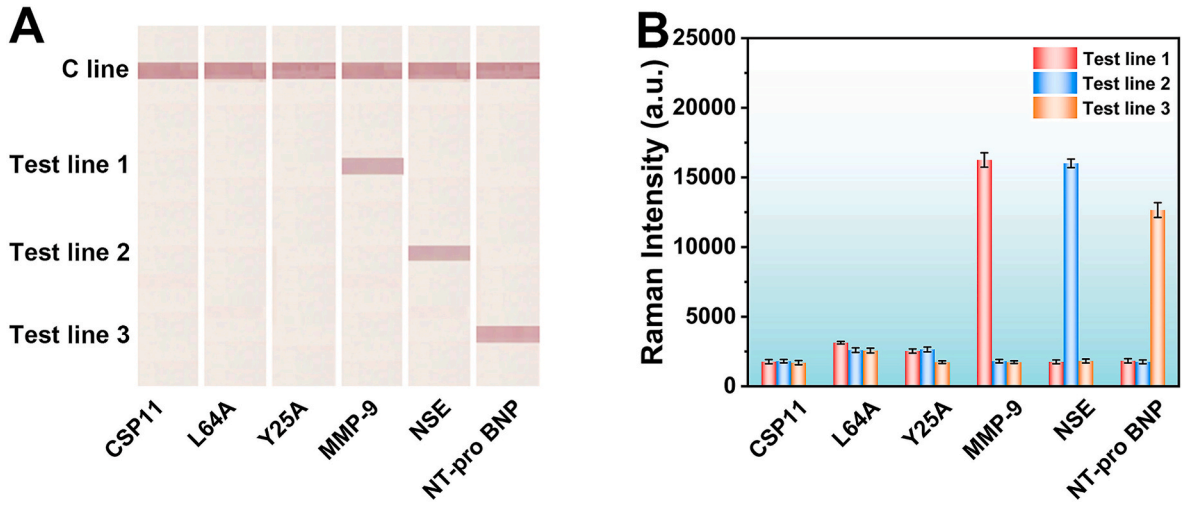

Fig. 6. Optical photographs (A) and corresponding specificity spectra of SERS-based LFIA strips with CSP11, L64A, Y25A, MMP-9, NSE and NT-pro BNP as target antigens at a concentration of 100 ng mL^{-1} (B).

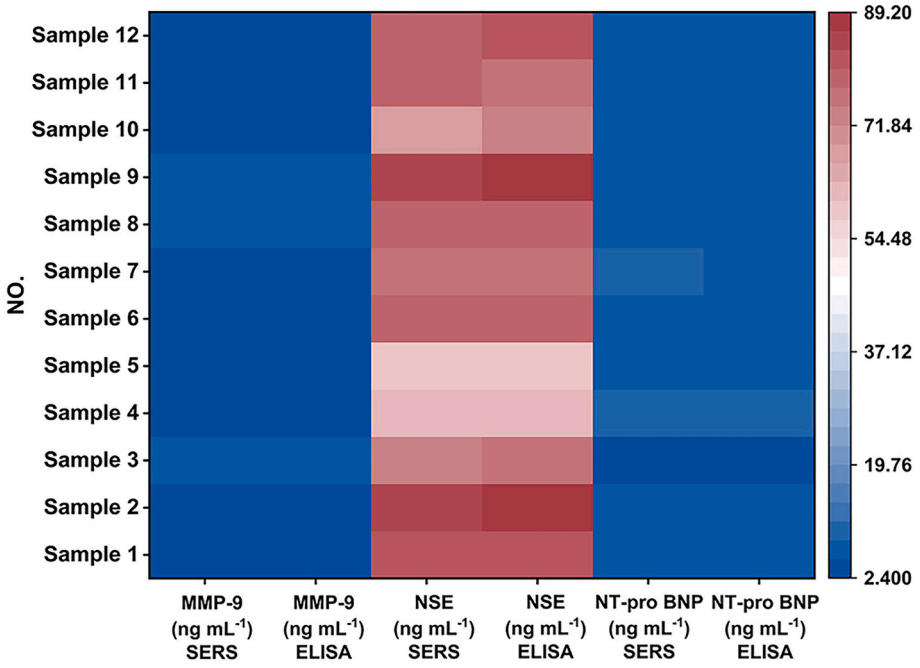

Fig. 7. The heatmap for MMP-9, NSE and NT-pro BNP concentration in clinical serum samples shows less color difference between SERS and ELISA ways in each protein.

with decreasing target antigen concentrations, until complete disappearance below 0.1 ng mL^{-1} for MMP-9, 1 ng mL^{-1} for NSE, and 1 ng mL^{-1} for NT-pro BNP. C-lines consistently showed color, confirming proper functioning of SERS strips. Visible limits of detection (vLODs) based on SERS-based LFIA were determined as 0.1 ng mL^{-1}, 1 ng mL^{-1}, and 1 ng mL^{-1} for MMP-9, NSE, and NT-pro BNP, respectively. Raman spectra analysis (Fig. 4D–F) indicated a linear relationship from 0.001 to 100 ng mL^{-1} for all three antigens, with regression equations of $y = 2634.54\log [C_{MMP\text{-}9}] + 10344.35$ ($R^2 = 0.9946$), $y = 2579.05\log [C_{NSE}] + 10378.05$ ($R^2 = 0.9946$), and $y = 1947.95\log [C_{NT\text{-}pro\ BNP}] + 8218.45$ ($R^2 = 0.9949$) (Fig. 4G–I). Limits of detection (LODs) were calculated as 0.00020 ng mL^{-1} for MMP-9, 0.00016 ng mL^{-1} for NSE, and 0.00012 ng mL^{-1} for NT-pro BNP, demonstrating satisfactory sensitivity compared to recent methods [37–48], as shown in Fig. 5 and the corresponding data were collected in Tabel S1. The calculated LOD was determined based on the formulas $LOD = 3\sigma/k$, where σ is the standard deviation of the blank samples, and k is the slope of the calibration curve.

3.5. Selectivity and specificity of the SERS-based LFIA for stroke biomarker detection

The specificity of SERS-based LFIA directly impacts the accuracy of simultaneous detection of the three biomarkers. Evaluation of specificity involved monitoring several interfering proteins (CSP11, L64A, Y25A, NT-pro BNP, NSE, and MMP-9 at 100 ng mL^{-1}). Target antigens produced distinct color bands exclusively on the test lines coated with corresponding antibodies, while interfering proteins showed no visible signal (Fig. 6A). Control lines consistently displayed color, validating experimental results. SERS signal results corroborated strip visualization (Fig. 6B), confirming effective differentiation of target markers from interfering antigens and high specificity and selectivity in detecting three stroke biomarkers. Repeatability of SERS-based LFIA was confirmed by detecting SERS signals of 10 ng mL^{-1} antigen solutions, showing intra-batch RSD values of 3.56 %, 2.80 %, and 2.90 % (Fig. S8A), and inter-batch RSD values of 5.95 %, 6.60 %, and 6.55 % (Fig. S8B), respectively, indicating good reproducibility and reliability.

3.6. Clinical serum samples analysis

The proposed SERS-based LFIA demonstrated excellent sensitivity and selectivity in detecting three stroke biomarkers. Clinical serum samples from 12 stroke patients were analyzed and compared with conventional ELISA to validate the practicality of the assay. Results obtained via SERS analysis were highly consistent with ELISA results, demonstrating that SERS-based LFIA can rapidly detect stroke biomarkers with accuracy comparable to established methods. As shown in Fig. 7, same results were shown as same color, warm colors to indicate large values and cool colors to indicate small values. This color representation of the numbers makes the data more intuitive and the contrast more obvious. Additionally, we processed 10 serum samples from non-stroke patients using our method. The concentrations of MMP-9 and NT-pro BNP in these samples, as shown in Fig. S9, were significantly lower compared to those of stroke patients. The results obtained for the non-stroke patients fell within the linear range of our method. Furthermore, the method's capability to simultaneously detect multiple biomarkers with minimal sample volume facilitates efficient patient screening, early diagnosis, and timely intervention (analysis time: 10–15 min), offering significant benefits in clinical settings. Compared to ELISA, SERS-based LFIA requires no specialized sample purification or extensive procedural steps, thus presenting an easier operational approach. Consequently, SERS-based LFIA holds promise as an effective method for rapid and accurate POCT in the future.

4. Conclusion

A novel SERS-based LFIA method has been successfully proposed for simultaneous detection of multiple biomarkers, demonstrating high sensitivity and ease of use. This advancement in the POCT system utilizing SERS-based LFIA strips facilitates rapid, sensitive, and multiplex detection of stroke biomarkers. The LODs for MMP-9, NSE, and NT-pro BNP were 0.00020 ng mL^{-1}, 0.00016 ng mL^{-1}, and 0.00012 ng mL^{-1}, respectively. Our SERS-based LFIA method demonstrates markedly lower detection limits in comparison to previously published methods, and its feasibility was confirmed through analysis of serum samples from 12 stroke patients. In comparison to ELISA, the developed SERS-based LFIA method offers superior speed and simplicity. Given the significance of MMP-9, NSE, and NT-pro BNP as critical biomarkers for stroke, this highly sensitive and effective immunoassay based on SERS shows potential as an innovative POCT approach for rapid stroke diagnosis.

CRediT authorship contribution statement

Yutong Wang: Writing – original draft, Software, Investigation, Data curation. **Qianchun Zhang:** Writing – original draft, Software, Resources, Data curation. **Mengping Huang:** Validation, Methodology. **Ganggang Ai:** Validation, Methodology. **Xiaofeng Liu:** Validation, Methodology. **Yuqi Zhang:** Writing – review & editing, Project administration, Funding acquisition. **Ran Li:** Writing – review & editing, Writing – original draft, Project administration, Funding acquisition, Conceptualization. **Jie Wu:** Writing – review & editing, Project administration, Funding acquisition.

Declaration of competing interest

The authors declare that they have no known competing financial interests or personal relationships thatcould have appeared to influence the work reported in this paper.

Acknowledgement

The authors gratefully acknowledge National Natural Science Foundation of China (NSFC) (Nos. 21663032, 31701679, 81703636), Open Sharing Platform for Scientific and Technological Resources of Shaanxi Province (No. 2021 PT-004), Natural Science Fundamental Research Program Key Projects of Shaan-xi Province (No. 2020QFY09-03), Municipal Special Fund of Yan'an for Outstanding Talented (No. 2019–18), Yan'an University Foundation for Talents Introduction (Nos. YDBK2015-11, YDBK2019-32). Guangxi First-class Disciplines (Agricultural Resources and Environment), Qinchuangyuan Introduces High-level Innovative Entrepreneurial Talent Projects QCYRCXM-2022-366, Yan'an Municipal Foundation for Multiscale Materials omics and Its Applications Interdisciplinary Science and Technology Innovation Team, Yan'an Municipal Key Industrial Chain Projects (No. 2022SLZDCY-013).

Appendix A. Supplementary data

Supplementary data to this article can be found online at https://doi.org/10.1016/j.talanta.2024.127166.

Data availability

Data will be made available on request.

References

[1] C.O. Johnson, M. Nguyen, G.A. Roth, E. Nichols, T. Alam, D. Abate, F. Abd-Allah, A. Abdelalim, H.N. Abraha, N.M.E. Abu-Rmeileh, O.M. Adebayo, A.M. Adeoye, G. Agarwal, S. Agrawal, A.N. Aichour, I. Aichour, M.T.E. Aichour, F. Alahdab, R. Ali, N. Alvis-Guzman, N.H. Anber, M. Anjomshoa, J. Arabloo, A. Arauz, J. Ärnlöv, A. Arora, A. Awasthi, M. Banach, M.A. Barboza, S.L. Barker-Collo, T. W. Bärnighausen, S. Basu, A.B. Belachew, Y.M. Belayneh, D.A. Bennett, I. M. Bensenor, K. Bhattacharyya, B. Biadgo, A. Bijani, B. Bikbov, M.S. Bin Sayeed, Z.

A. Butt, L. Cahuana-Hurtado, J.J. Carrero, F. Carvalho, C.A. Castañeda-Orjuela, F. Castro, F. Catalá-López, Y. Chaiah, P.P.-C. Chiang, J.-Y.J. Choi, H. Christensen, D.-T. Chu, M. Cortinovis, A.A.M. Damasceno, L. Dandona, R. Dandona, A. Daryani, K. Davletov, B. de Courten, V. De la Cruz-Góngora, M.G. Degefa, S.D. Dharmaratne, D. Diaz, M. Dubey, E.E. Duken, D. Edessa, M. Endres, E.J.A. Faraon, F. Farzadfar, E. Fernandes, F. Fischer, L.S. Flor, M. Ganji, A.K. Gebre, T.G. Gebremichael, B. Geta, K.E. Gezae, P.S. Gill, E.V. Gnedovskaya, H. Gómez-Dantés, A.C. Goulart, G. Grosso, Y. Guo, R. Gupta, A. Haj-Mirzaian, A. Haj-Mirzaian, S. Hamidi, G. J. Hankey, H.Y. Hassen, S.I. Hay, M.I. Hegazy, B. Heidari, N.A. Herial, M. A. Hosseini, S. Hostiuc, S.S.N. Irvani, S.M.S. Islam, N. Jahanmehr, M. Javanbakht, R.P. Jha, J.B. Jonas, J.J. Jozwiak, M. Jürisson, A. Kahsay, R. Kalani, Y. Kalkonde, T. A. Kamil, T. Kanchan, A. Karch, N. Karimi, H. Karimi-Sari, A. Kasaeian, T.D. Kassa, H. Kazemeini, A.T. Kefale, Y.S. Khader, I.A. Khalil, E.A. Khan, Y.-H. Khang, J. Khubchandani, D. Kim, Y.J. Kim, A. Kisa, M. Kivimäki, A. Koyanagi, R. K. Krishnamurthi, G.A. Kumar, A. Lafranconi, S. Lewington, S. Li, W.D. Lo, A. D. Lopez, S. Lorkowski, P.A. Lotufo, M.T. Mackay, M. Majdan, R. Majdzadeh, A. Majeed, R. Malekzadeh, N. Manafi, M.A. Mansournia, M.M. Mehndiratta, V. Mehta, G. Mengistu, A. Meretoja, T.J. Meretoja, B. Miazgowski, T. Miazgowski, T.R. Miller, E.M. Mirrakhimov, B. Mohajer, Y. Mohammad, M. Mohammadoo-khorasani, S. Mohammed, F. Mohebi, A.H. Mokdad, Y. Mokhayeri, G. Moradi, L. Morawska, I. Moreno Velásquez, S.M. Mousavi, O.S.S. Muhammed, W. Muruet, M. Naderi, M. Naghavi, G. Naik, B.R. Nascimento, R.I. Negoi, C.T. Nguyen, L. H. Nguyen, Y.L. Nirayo, B. Norrving, J.J. Noubiap, R. Ofori-Asenso, F.A. Ogbo, A. T. Olagunju, T.O. Olagunju, M.O. Owolabi, J.D. Pandian, S. Patel, N. Perico, M. A. Piradov, S. Polinder, M.J. Postma, H. Poustchi, V. Prakash, M. Qorbani, A. Rafiei, F. Rahim, K. Rahimi, V. Rahimi-Movaghar, M. Rahman, M.A. Rahman, C. Reis, G. Remuzzi, A.M.N. Renzaho, S. Ricci, N.L.S. Roberts, S.R. Robinson, L. Roever, G. Roshandel, P. Sabbagh, H. Safari, S. Safari, S. Safiri, A. Sahebkar, S. Salehi Zahabi, A.M. Samy, P. Santalucia, I.S. Santos, J.V. Santos, M.M. Santric Milicevic, B. Sartorius, A.R. Sawant, A.E. Schutte, S.G. Sepanlou, A. Shafieesabet, M.A. Shaikh, M. Shams-Beyranvand, A. Sheikh, K.N. Sheth, K. Shibuya, M. Shigematsu, M.-J. Shin, I. Shiue, S. Siabani, B.H. Sobaih, L.A. Sposato, I. Sutradhar, P.N. Sylaja, C.E.I. Szoeke, B.J. Te Ao, M.-H. Temsah, O. Temsah, A. G. Thrift, M. Tonelli, R. Topor-Madry, B.X. Tran, K.B. Tran, T.C. Truelsen, A. G. Tsadik, I. Ullah, O.A. Uthman, M. Vaduganathan, P.R. Valdez, T.J. Vasankari, R. Vasanthan, N. Venketasubramanian, K. Vosoughi, G.T. Vu, Y. Waheed, E. Weiderpass, K.G. Weldegwergs, R. Westerman, C.D.A. Wolfe, D.Z. Wondafrash, G. Xu, A. Yadollahpour, T. Yamada, H. Yatsuya, E.M. Yimer, N. Yonemoto, M. Yousefifard, C. Yu, Z. Zaidi, M. Zamani, A. Zarghi, Y. Zhang, S. Zodpey, V. L. Feigin, T. Vos, C.J.L. Murray, Global, regional, and national burden of stroke, 1990-2016: a systematic analysis for the Global Burden of Disease Study 2016, Lancet Neurol. 18 (2019) 439–458, https://doi.org/10.1016/s1474-4422(19)30034-1.

[2] M.O. Owolabi, A.G. Thrift, A. Mahal, M. Ishida, S. Martins, W.D. Johnson, J. Pandian, F. Abd-Allah, J. Yaria, H.T. Phan, G. Roth, S.L. Gall, R. Beare, T. G. Phan, R. Mikulik, R.O. Akinyemi, B. Norrving, M. Brainin, V.L. Feigin, C. Abanto, S.F. Abera, A. Addissie, O. Adebayo, A.O. Adeleye, Y. Adilbekov, B. Adilbekova, T.A. Adoukonou, D. Aguiar de Sousa, T. Ajagbe, Z. Akhmetzhanova, A. Akpalu, J. Álvarez Ahlgren, S. Ameriso, S. Andonova, F.E. Awoniyi, M. Bakhiet, M. Barboza, H. Basri, P. Bath, O. Bello, D. Bereczki, S. Beretta, A. Berkowitz, A. Bernabé-Ortiz, J. Bernhardt, G. Berzina, M. Bisharyan, P. Bovet, H. Budincevic, D. Cadilhac, V. Caso, C. Chen, J. Chin, K. Chwojnicki, A. Conforto, V.T. Cruz, M. D'Amelio, K. Danielyan, S. Davis, V. Demarin, R. Dempsey, M. Dichgans, K. Dokova, G. Donnan, M.S. Elkind, M. Endres, U. Fischer, F. Gankpé, A. Gaye Saavedra, A. Gil, M. Giroud, E. Gnedovskaya, V. Hachinski, M. Hafdi, R. Hamadeh, T.K. Hamzat, G. Hankey, M. Heldner, E.A. Ibrahim, N.M. Ibrahim, M. Inoue, S. Jee, J.-S. Jeng, Y. Kalkonde, S. Kamenova, B. Karaszewski, P. Kelly, T. Khan, S. Kiechl, A. Kondybayeva, J. Kõrv, M. Kravchenko, R.V. Krishnamurthi, J. Kruja, M. Lakkhanaloet, P. Langhorne, P.M. Lavados, Z.K. Law, A. Lawal, M. Lazo-Porras, D. Lebedynets, T.-H. Lee, T. Leung, D.S. Liebeskind, P. Lindsay, P. López-Jaramillo, P.A. Lotufo, J. Machline-Carrion, A. Makanjuola, H.S. Markus, J.M. Marquez-Romero, M. Medina, S. Medukhanova, M.M. Mehndiratta, A. Merkin, E. Mirrakhimov, S. Mohl, M. Moscoso-Porras, A. Müller-Stierlin, S. Murphy, K. I. Musa, A. Nasreldein, R.G. Nogueira, C. Nolte, J.J. Noubiap, N. Novarro-Escudero, Y. Ogun, R.A. Oguntoye, M.I. Oraby, M. Osundina, B. Ovbiagele, D.N. Orken, A.Ö. Ozdemir, S. Ozturk, M. Paccot, J. Phromjai, P. Piradov, T. Platz, T. Potpara, A. Ranta, F. Rathore, E. Richard, R.L. Sacco, R. Sahathevan, I. Santos Carquín, G. Saposnik, F.S. Sarfo, M. Sharma, K. Sheth, A. Shobhana, N. Suwanwela, I. Svyato, P.N. Sylaja, X. Tao, K.T. Thakur, D. Toni, M.A. Topcuoglu, J. Torales, A. Towfighi, T.C. Truelsen, A. Tsiskaridze, M. Tulloch-Reid, N. Useche, P. Vanacker, S. Vassilopoulou, G. Vukorepa, V. Vuletic, K.W. Wahab, W. Wang, T. Wijeratne, C. Wolfe, Y.M. Yifru, A. Yock-Corrales, N. Yonemoto, L. Yperzeele, P. Zhang, Primary stroke prevention worldwide: translating evidence into action, Lancet Public Health 7 (2022) 74–85, https://doi.org/10.1016/s2468-2667(21)00230-9.

[3] B.C.V. Campbell, D.A. De Silva, M.R. Macleod, S.B. Coutts, L.H. Schwamm, S. M. Davis, G.A. Donnan, Ischaemic stroke, Nat. Rev. Dis. Primers 5 (2019), https://doi.org/10.1038/s41572-019-0118-8.

[4] V.L. Feigin, M.O. Owolabi, V.L. Feigin, F. Abd-Allah, R.O. Akinyemi, N. V. Bhattacharjee, M. Brainin, J. Cao, V. Caso, B. Dalton, A. Davis, R. Dempsey, J. Duprey, W. Feng, G.A. Ford, S. Gall, D. Gandhi, D.C. Good, V. Hachinski, W. Hacke, G.J. Hankey, M. Ishida, W. Johnson, J. Kim, P. Lavados, P. Lindsay, A. Mahal, S. Martins, C. Murray, T.P. Nguyen, B. Norrving, M.T. Olaiya, O. V. Olalusi, J. Pandian, H. Phan, T. Platz, A. Ranta, S. Rehman, G. Roth, I. A. Sebastian, A.E. Smith, N.C. Suwanwela, P.N. Sylaja, R. Thapa, A.G. Thrift, E. Uvere, S.E. Vollset, D. Yavagal, J. Yaria, M.O. Owolabi, M.O. Owolabi, V. L. Feigin, F. Abd-Allah, S.F. Abera, R. Akinyemi, M. Brainin, V. Caso, R.J. Dempsey, G.A. Ford, S. Gall, D. Gandhi, V. Hachinski, W. Hacke, G.J. Hankey, N.M. Ibrahim, W. Johnson, P. Lavados, L. Liu, P. Lindsay, S. Martins, B. Norrving, M.T. Olaiya, B. Ovbiagele, J. Pandian, H. Phan, M. Piradov, T. Platz, A. Ranta, G. Roth, I. A. Sebastian, N. Suwanwela, P.N. Sylaja, A.G. Thrift, E. Uvere, J. Yaria, C. Abanto, A. Addissie, A.O. Adeleye, Y. Adilbekov, B. Adilbekova, T.A. Adoukonou, D. Aguiar de Sousa, Z. Akhmetzhanova, A. Akpalu, M. El Alaoui-Faris, S.F. Ameriso, S. Andonova, A. Arsovska, F.E. Awoniyi, M. Bakhiet, M.A. Barboza, H. Basri, P. M. Bath, D. Bereczki, S. Beretta, A.L. Berkowitz, J. Bernhardt, G. Berzina, B. Bhavsar, M.S. Bisharyan, M. Bohara, P. Bovet, H. Budincevic, D.A. Cadilhac, D. Čerimagić, A. Charway-Felli, C. Chen, J.H. Chin, H. Christensen, K. Chwojnicki, A.B. Conforto, M. Correia, D.L. Mora Cuervo, A. Członkowska, M. D'Amelio, K. E. Danielyan, S. Davis, V. Demarin, A.M. Demchuk, M. Dichgans, K. Dokova, G. Donnan, J.C. Duran, G. Ekeng, M.S. Elkind, M. Endres, U. Fischer, Y. Flomin, F. Gankpe, M. Gavidia, A. Gaye Saavedra, M. Gebreyohanns, M. George, M. Gierlotka, M. Giroud, E.V. Gnedovskaya, I.P. Gonçalves, F. Gongora-Rivera, P. S. Gunaratne, R.R. Hamadeh, T.-h. K. Hamzat, M.R. Heldner, E. Ibrahim, H. Ihle-Hansen, S. Jee, J. Jiann-Shing, S.C. Johnston, D. Jovanovic, K. Jurjāns, R. Kalani, Y. Kalkonde, S. Kamenova, B. Karaszewski, P. Kelly, S. Kiechl, A. Kondybayeva, J. Kõrv, G. Kozera, M. Kravchenko, Y. Krespi, R. Krishnamurthi, J. Kruja, K. Kutluk, P. Langhorne, Z.K. Law, D. Lebedynets, T.-H. Lee, T.W. Leung, D.S. Liebeskind, P. López-Jaramillo, P.A. Lotufo, M.J. Machline-Carrion, L.F. Maia, B. Malojcic, H. S. Markus, J.M. Marquez-Romero, M.T. Medina, S. Medukhanova, M. M. Mehndiratta, E. Miglāne, I. Mihejeva, R. Mikulik, E. Mirrakhimov, S. Mohl, S. Munakomi, S. Murphy, K.I. Musa, A. Nasreldein, R.G. Nogueira, C.H. Nolte, J. J. Noubiap, N. Novarro-Escudero, C. Ocampo, M. O'Donnell, Y. Ogun, A. Ogunniyi, M.I. Oraby, D.N. Õrken, A.O. Özdemir, S. Ozturk, M. Paccot, T. Pereira, A. Peeters, T. Potpara, H. Proios, F.A. Rathore, R.L. Sacco, R. Sahathevan, E.S. Sandset, I. Renato Santos, G. Saposnik, F.S. Sarfo, J. Sargento-Freitas, M. Sharma, L. Shaw, K.N. Sheth, Y.-I. Shin, A. Shobhana, S.N. Silva, V. Tedim Cruz, K. Thakur, L. J. Thapa, D. Toni, M.A. Topcuoglu, J. Torales, A. Towfighi, T. Truelsen, A. Tsiskaridze, M. Tulloch-Reid, J.N. Useche, P. Vanacker, S. Vassilopoulou, G. Vukorepa, V. Vuletic, K.W. Wahab, W. Wang, T. Wijeratne, B. Wojtyniak, C. Wolfe, M.N. Yacouba, J. Yang, Y.M. Yifru, A. Yock-Corrales, N. Yonemoto, L. Yperzeele, P. Zagożdżon, Pragmatic solutions to reduce the global burden of stroke: a World stroke organization–lancet Neurology commission, Lancet Neurol. 22 (2023) 1160–1206, https://doi.org/10.1016/s1474-4422(23)00277-6.

[5] M. Brainin, W. Grisold, G.J. Hankey, B. Norrving, V.L. Feigin, Time to revise primary prevention guidelines for stroke and cardiovascular disease, Lancet Neurol. 21 (2022) 686–687, https://doi.org/10.1016/s1474-4422(22)00264-2.

[6] Q. Zhang, A. Wang, Q. Xu, X. Xia, X. Tian, Y. Zhang, X. Li, X. Yang, X. Wang, J. Peng, Y. Li, L. Liu, S. Jin, X. Meng, X. Zhao, Y. Wang, M. He, Q. Dong, G. Zhao, K. Chen, P. Xie, Y. Xu, Y. Yang, L. Guo, Y. Li, Y. Wang, X. Zhang, A. Xu, X. Pan, C. Xiao, D. Wang, H. Li, Y. Gao, J. Xia, H. Zhao, H. Wang, Y. He, W. Li, X. Wei, J. Bai, S. Cao, Y. Song, Z. Ma, N. Zhang, N. Yin, L. Zeng, L. Zhang, F. Yang, J. Zhang, J. Wang, H. Tang, Y. Li, H. Zhou, H. Feng, D. Song, J. Wang, Y. Ma, L. Chen, K. Xiao, Q. Zhai, J. Li, X. Li, Y. Yang, X. Mei, Z. Zhu, Y. Zhang, Y. Liu, H. Nie, B. Fu, G. Huang, G. Zeng, B. Liu, W. Xiaomin, L. Xu, F. Zhang, L. Wang, W. Han, S. Meng, C.e. Xiao, Z. Yang, Y. Deng, H. Ying, L. Tang, C. Jia, C. Li, S. Liu, M. Han, Y. Zhang, F. Peng, J. Zhao, D. Qiao, W. Li, S. Cai, Q. Song, C. Xiao, M. Chen, J. Lei, A. Cai, W. Xu, J. Cao, X. Liu, D. Tan, T. Feng, F. Lina, H. Yan, C. Liu, Y. Wang, Q. Yang, L. Ji, J. Xu, L. Chen, S. Chen, Y. Song, L. Mei, S. Ouyang, J. Li, D. Zhao, Z. Dong, W. Jin, G. Tang, N. Geng, H. Cai, Z. Li, Y. Chen, L. Huang, Y. Zhang, P. Lei, M. Yan, X. Zhang, Y. Wang, H. Dou, K. Wang, G. Nie, Efficacy and safety of ginkgo diterpene lactone meglumine in acute ischemic stroke, JAMA Netw. Open 6 (2023) 2328828, https://doi.org/10.1001/jamanetworkopen.2023.28828.

[7] H. Kawano, A. Bivard, L. Lin, H. Ma, X. Cheng, R. Aviv, B. O'Brien, K. Butcher, M. Lou, J. Zhang, J. Jannes, Q. Dong, C.R. Levi, M.W. Parsons, Perfusion computed tomography in patients with stroke thrombolysis, Brain (2016) 338, https://doi.org/10.1093/brain/aww338.

[8] S.K. UmaMaheswaran, F. Ahmad, R. Hegde, A.M. Alwakeel, S. Rameem Zahra, Enhanced non-contrast computed tomography images for early acute stroke detection using machine learning approach, Expert Syst. Appl. 240 (2024) 122559, https://doi.org/10.1016/j.eswa.2023.122559.

[9] Y. Liu, A.T.L. Leong, Y. Zhao, L. Xiao, H.K.F. Mak, A.C.O. Tsang, G.K.K. Lau, G.K. K. Leung, E.X. Wu, A low-cost and shielding-free ultra-low-field brain MRI scanner, Nat. Commun. 12 (2021) 7238, https://doi.org/10.1038/s41467-021-27317-1.

[10] W. Xu, J. Lin, M. Gao, Y. Chen, J. Cao, J. Pu, L. Huang, J. Zhao, K. Qian, Rapid computer-aided diagnosis of stroke by serum metabolic fingerprint based multi-modal recognition, Adv. Sci. 7 (2020) 2002021, https://doi.org/10.1002/advs.202002021.

[11] M. Ribo, C.A. Molina, E. Cobo, N. Cerdà, A. Tomasello, H. Quesada, M.A. De Miquel, M. Millan, C. Castaño, X. Urra, L. Sanroman, A. Dàvalos, T. Jovin, E. Sanjuan, M. Rubiera, J. Pagola, A. Flores, M. Muchada, P. Meler, E. Huerga, S. Gelabert, P. Coscojuela, D. Rodriguez, E. Santamarina, O. Maisterra, S. Boned, L. Seró, A. Rovira, L. Muñoz, N. Pérez de la Ossa, M. Gomis, L. Dorado, E. López-Cancio, E. Palomeras, J. Munuera, P. García Bermejo, S. Remollo, R. García-Sort, P. Cuadras, P. Puyalto, M. Hernández-Pérez, M. Jiménez, A. Martínez-Piñeiro, G. Lucente, A. Chamorro, V. Obach, A. Cervera, S. Amaro, L. Llull, J. Codas, M. Balasa, J. Navarro, H. Ariño, A. Aceituno, S. Rudilosso, A. Renu, J.M. Macho, J. Blasco, A. López, N. Macías, P. Cardona, F. Rubio, L. Cano, B. Lara, L. Aja, A. Chamorro, J. Serena, A. Rovira, G. Albers, K. Lees, J. Arenillas, R. Roberts, M. Goyal, A.M. Demchuk, P. Minhas, F. Al-Ajlan, M. Salluzzi, L. Zimmel, S. Patel, M. Eesa, R. von Kummer, J. Martí-Fàbregas, B. Jankowitz, J. Serena, M. Salvat-Plana, E. López-Cancio, M. Hernandez-Pérez, Association between time to

reperfusion and outcome is primarily driven by the time from imaging to reperfusion, Stroke 47 (2016) 999–1004, https://doi.org/10.1161/strokeaha.115.011721.
[12] S.J. Kim, G.J. Moon, O.Y. Bang, Biomarkers for stroke, J. Stroke 15 (2013), https://doi.org/10.5853/jos.2013.15.1.27.
[13] A. Bustamante, E. López-Cancio, S. Pich, A. Penalba, D. Giralt, T. García-Berrocoso, C. Ferrer-Costa, T. Gasull, M. Hernández-Pérez, M. Millan, M. Rubiera, P. Cardona, L. Cano, H. Quesada, M. Terceño, Y. Silva, M. Castellanos, M. Garces, S. Reverté, X. Ustrell, R. Marés, J.J. Baiges, J. Serena, F. Rubio, E. Salas, A. Dávalos, J. Montaner, Blood biomarkers for the early diagnosis of stroke, Stroke 48 (2017) 2419–2425, https://doi.org/10.1161/strokeaha.117.017076.
[14] X. Chen, S. Zhou, Y. Wang, L. Zheng, S. Guan, D. Wang, L. Wang, X. Guan, Nanopore single-molecule analysis of biomarkers: providing possible clues to disease diagnosis, Trends Analyt. Chem. 162 (2023) 117060, https://doi.org/10.1016/j.trac.2023.117060.
[15] F. Iemolo, E. Sanzaro, G. Duro, A. Giordano, M. Paciaroni, The prognostic value of biomarkers in stroke, Immun. Ageing 13 (2016), https://doi.org/10.1186/s12979-016-0074-z.
[16] M. Gelderblom, T. Daehn, B. Schattling, P. Ludewig, C. Bernreuther, P. Arunachalam, J. Matschke, M. Glatzel, C. Gerloff, M.A. Friese, T. Magnus, Plasma levels of neuron specific enolase quantify the extent of neuronal injury in murine models of ischemic stroke and multiple sclerosis, Neurobiol. Dis. 59 (2013) 177–182, https://doi.org/10.1016/j.nbd.2013.07.017.
[17] A. Di Castelnuovo, G. Veronesi, S. Costanzo, T. Zeller, R.B. Schnabel, A. de Curtis, V. Salomaa, R. Borchini, M. Ferrario, S. Giampaoli, F. Kee, S. Söderberg, T. Niiranen, K. Kuulasmaa, G. de Gaetano, M.B. Donati, S. Blankenberg, L. Iacoviello, NT-proBNP (N-terminal pro-B-type natriuretic peptide) and the risk of stroke, Stroke 50 (2019) 610–617, https://doi.org/10.1161/strokeaha.118.023218.
[18] W. Nadruz, B.L. Claggett, J.J. McMurray, M. Packer, M.R. Zile, J.L. Rouleau, A. S. Desai, K. Swedberg, M. Lefkowitz, V.C. Shi, M.F. Prescott, S.D. Solomon, Impact of body mass index on the accuracy of N-terminal pro-brain natriuretic peptide and brain natriuretic peptide for predicting outcomes in patients with chronic heart failure and reduced ejection fraction, Circulation 134 (2016) 1785–1787, https://doi.org/10.1161/circulationaha.116.024976.
[19] L. Zhao, L. Li, Y. Zhao, C. Zhu, R. Yang, M. Fang, Y. Luan, Aptamer-based point-of-care-testing for small molecule targets: from aptamers to aptasensors, devices and applications, Trends Analyt. Chem. 169 (2023) 117408, https://doi.org/10.1016/j.trac.2023.117408.
[20] J. Qin, W. Wang, L. Gao, S.Q. Yao, Emerging biosensing and transducing techniques for potential applications in point-of-care diagnostics, Chem. Sci. 13 (2022) 2857–2876, https://doi.org/10.1039/d1sc06269g.
[21] Y. Liu, L. Zhan, Z. Qin, J. Sackrison, J.C. Bischof, Ultrasensitive and highly specific lateral flow assays for point-of-care diagnosis, ACS Nano 15 (2021) 3593–3611, https://doi.org/10.1021/acsnano.0c10035.
[22] A. Sena-Torralba, R. Álvarez-Diduk, C. Parolo, A. Piper, A. Merkoçi, Toward next generation lateral flow assays: integration of nanomaterials, Chem. Rev. 122 (2022) 14881–14910, https://doi.org/10.1021/acs.chemrev.1c01012.
[23] S. Cavalera, B. Colitti, G.M.D. Mia, F. Feliziani, S.D. Giudici, P.P. Angioi, F. D'Errico, D. Scalas, A. Scollo, T. Serra, M. Chiarello, V. Testa, F.D. Nardo, C. Baggiani, A. Oggiano, S. Rosati, L. Anfossi, Development of molecular and antigenic-based rapid tests for the identification of African swine fever virus in different tissues, Talanta 258 (2023) 124443, https://doi.org/10.1016/j.talanta.2023.124443.
[24] J. Guo, S. Chen, J. Guo, X. Ma, Nanomaterial labels in lateral flow immunoassays for point-of-care-testing, J. Mater. Sci. Technol. 60 (2021) 90–104, https://doi.org/10.1016/j.jmst.2020.06.003.
[25] M. You, M. Lin, Y. Gong, S. Wang, A. Li, L. Ji, H. Zhao, K. Ling, T. Wen, Y. Huang, D. Gao, Q. Ma, T. Wang, A. Ma, X. Li, F. Xu, Household fluorescent lateral flow strip platform for sensitive and quantitative prognosis of heart failure using dual-color upconversion nanoparticles, ACS Nano 11 (2017) 6261–6270, https://doi.org/10.1021/acsnano.7b02466.
[26] G. Guo, T. Zhao, R. Sun, M. Song, H. Liu, S. Wang, J. Li, J. Zeng, Au-Fe_3O4 dumbbell-like nanoparticles based lateral flow immunoassay for colorimetric and photothermal dual-mode detection of SARS-CoV-2 spike protein, Chin. Chem. Lett. 35 (2024) 109198, https://doi.org/10.1016/j.cclet.2023.109198.
[27] X. Chen, Y. Leng, L. Hao, H. Duan, J. Yuan, W. Zhang, X. Huang, Y. Xiong, Self-assembled colloidal gold superparticles to enhance the sensitivity of lateral flow immunoassays with sandwich format, Theranostics 10 (2020) 3737–3748, https://doi.org/10.7150/thno.42364.
[28] R. Shu, S. Liu, M. Wang, M. Zhang, B. Wang, K. Wang, I.A. Darwish, J. Wang, D. Zhang, Dual-plasmonic CuS@Au heterojunctions synergistic enhanced photothermal and colorimetric dual signal for sensitive multiplexed LFIA, Biosens. Bioelectron. 255 (2024) 116235, https://doi.org/10.1016/j.bios.2024.116235.
[29] C. Chen, B. Huang, W. Xu, R. Hou, B. Dong, X. Yu, Z. Wang, H. Li, Enhancing the stability and sensitivity of a lateral flow immunoassay using stabilized AuNPs for the simultaneous detection of sulfonamides and antibacterial synergists in chicken meat, Sens. Actuators B Chem. 412 (2024) 135812, https://doi.org/10.1016/j.snb.2024.135812.
[30] H. Gong, S. Gai, Y. Tao, Y. Du, Q. Wang, A.A. Ansari, H. Ding, Q. Wang, P. Yang, Colorimetric and photothermal dual-modal switching lateral flow immunoassay based on a forced dispersion prussian blue nanocomposite for the sensitive detection of prostate-specific antigen, Anal. Chem. 96 (2024) 8665–8673, https://doi.org/10.1021/acs.analchem.4c00862.
[31] T. Gong, C.M. Das, M.-J. Yin, T.-R. Lv, N.M. Singh, A.M. Soehartono, G. Singh, Q.-F. An, K.-T. Yong, Development of SERS tags for human diseases screening and detection, Coord. Chem. Rev. 470 (2022) 214711, https://doi.org/10.1016/j.ccr.2022.214711.
[32] C. Zong, M. Xu, L.J. Xu, T. Wei, X. Ma, X.S. Zheng, R. Hu, B. Ren, Surface-enhanced Raman spectroscopy for bioanalysis: reliability and challenges, Chem. Rev. 118 (2018) 4946–4980, https://doi.org/10.1021/acs.chemrev.7b00668.
[33] T. Zhao, P. Liang, J. Ren, J. Zhu, X. Yang, H. Bian, J. Li, X. Cui, C. Fu, J. Xing, C. Wen, J. Zeng, Gold-silver alloy hollow nanoshells-based lateral flow immunoassay for colorimetric, photothermal, and SERS tri-mode detection of SARS-CoV-2 neutralizing antibody, Anal. Chim. Acta 1255 (2023) 341102, https://doi.org/10.1016/j.aca.2023.341102.
[34] J. Liang, L. Wu, Y. Wang, W. Liang, Y. Hao, M. Tan, G. He, D. Lv, Z. Wang, T. Zeng, X. Zhang, C. Lu, Q. Song, B. Peng, J. Zhao, B. Zhu, Y. Tang, SERS/photothermal-based dual-modal lateral flow immunoassays for sensitive and simultaneous antigen detection of respiratory viral infections, Sens. Actuators B Chem. 389 (2023) 133875, https://doi.org/10.1016/j.snb.2023.133875.
[35] S. Atta, Y. Zhao, J.Q. Li, T. Vo-Dinh, Dual-Modal Colorimetric and Surface-enhanced Raman scattering (SERS)-based lateral flow immunoassay for ultrasensitive detection of SARS-CoV-2 using a plasmonic gold nanocrown, Anal. Chem. 96 (2024) 4783–4790, https://doi.org/10.1021/acs.analchem.3c04361.
[36] X. Liu, X. Su, M. Chen, Y. Xie, M. Li, Self-calibrating surface-enhanced Raman scattering-lateral flow immunoassay for determination of amyloid-β biomarker of Alzheimer's disease, Biosens. Bioelectron. 245 (2024) 115840, https://doi.org/10.1016/j.bios.2023.115840.
[37] E. Shabani, M.J. Abdekhodaie, S.A. Mousavi, F. Taghipour, ZnO nanoparticle/nanorod-based label-free electrochemical immunoassay for rapid detection of MMP-9 biomarker, Biochem. Eng. J. 164 (2020) 107772, https://doi.org/10.1016/j.bej.2020.107772.
[38] S. Jing, B. Yu, H. Qiao, Y. Huang, X. Liao, Development of electrochemical sensor for coronary heart disease biomarker MMP-9 analysis, Int. J. Electrochem. Sci. 12 (2017) 5233–5242, https://doi.org/10.20964/2017.06.45.
[39] M. Ben Ismail, E. de la Serna, G. Ruiz-Vega, T. García-Berrocoso, J. Montaner, M. Zourob, A. Othmane, E. Baldrich, Using magnetic beads and signal amplifiers to produce short and simple immunoassays: application to MMP-9 detection in plasma samples, Anal. Chim. Acta 999 (2018) 144–154, https://doi.org/10.1016/j.aca.2017.11.013.
[40] G. Ruiz-Vega, A. García-Robaina, M. Ben Ismail, H. Pasamar, T. García-Berrocoso, J. Montaner, M. Zourob, A. Othmane, F.J. del Campo, E. Baldrich, Detection of plasma MMP-9 within minutes. Unveiling some of the clues to develop fast and simple electrochemical magneto-immunosensors, Biosens. Bioelectron. 115 (2018) 45–52, https://doi.org/10.1016/j.bios.2018.05.020.
[41] H. Wang, M. Wang, H. Wang, X. Ren, H. Wang, Q. Wei, D. Wu, Detection of NSE by a photoelectrochemical self-powered immunosensor integrating RGO photocathode and WO_3/Mn:CdS nanomaterial photoanode, Biosens. Bioelectron. 207 (2022) 114196, https://doi.org/10.1016/j.bios.2022.114196.
[42] Y. Tang, X. Hu, Y. Liu, Y. Chen, F. Zhao, B. Zeng, An antifouling electrochemiluminescence sensor based on mesoporous CuO_2@SiO_2/luminol nanocomposite and co-reactant of ionic liquid functionalized boron nitride quantum dots for ultrasensitive NSE detection, Biosens. Bioelectron. 214 (2022) 114492, https://doi.org/10.1016/j.bios.2022.114492.
[43] L. Ao, T. Liao, L. Huang, S. Lin, K. Xu, J. Ma, S. Qiu, X. Wang, Q. Zhang, Sensitive and simultaneous detection of multi-index lung cancer biomarkers by an NIR-II fluorescence lateral-flow immunoassay platform, Chem. Eng. J. 436 (2022) 135204, https://doi.org/10.1016/j.cej.2022.135204.
[44] Y. Fan, J. Liu, Y. Wang, J. Luo, H. Xu, S. Xu, X. Cai, A wireless point-of-care testing system for the detection of neuron-specific enolase with microfluidic paper-based analytical devices, Biosens. Bioelectron. 95 (2017) 60–66, https://doi.org/10.1016/j.bios.2017.04.003.
[45] A. Sinha, T.-Y. Tai, K.-H. Li, P. Gopinathan, Y.-D. Chung, I. Sarangadharan, H.-P. Ma, P.-C. Huang, S.-C. Shiesh, Y.-L. Wang, G.-B. Lee, An integrated microfluidic system with field-effect-transistor sensor arrays for detecting multiple cardiovascular biomarkers from clinical samples, Biosens. Bioelectron. 129 (2019) 155–163, https://doi.org/10.1016/j.bios.2019.01.001.
[46] Y. Zhuo, W.-J. Yi, W.-B. Lian, R. Yuan, Y.-Q. Chai, A. Chen, C.-M. Hu, Ultrasensitive electrochemical strategy for NT-proBNP detection with gold nanochains and horseradish peroxidase complex amplification, Biosens. Bioelectron. 26 (2011) 2188–2193, https://doi.org/10.1016/j.bios.2010.09.033.
[47] H. Li, X. Yin, D. Sun, K. Xia, C. Kang, S. Chu, P. Zhang, H. Wang, Y. Qiu, Detection of NT-pro BNP using fluorescent protein modified by streptavidin as a label in immunochromatographic assay, Sensing and Bio-Sensing Research 11 (2016) 1–7, https://doi.org/10.1016/j.sbsr.2016.08.001.
[48] K.-S. Song, S. Nimse, M. Sonawane, S. Warkad, T. Kim, Ultra-sensitive NT-proBNP quantification for early detection of risk factors leading to heart failure, Sensors 17 (2017) 2116, https://doi.org/10.3390/s17092116.